Multi-Level Gated U-Net for Denoising TMR Sensor-Based MCG Signals

Zeyu Xing[2*], Hao Li[3*], Hao Dou[4], Zhong Zheng[1], Jingguo Dai[5], Chen Wang[5], Jian Cui[5(✉)], Xin Zhang[1], and Tianzi Jiang[1]

[1] Beijing Key Laboratory of Brainnetome and Brain-Computer Interface, Institute of Automation, Chinese Academy of Sciences, Beijing, China
[2] School of Management, Zhejiang University, Hangzhou, China
[3] School of Biomedical Engineering & State Key Laboratory of Advanced Medical Materials and Devices, ShanghaiTech University, Shanghai, China
[4] Shanghai University of Finance and Economics, Shanghai, China
[5] Zhejiang Lab, Hangzhou, China
cuijian@zhejianglab.com

Abstract. Tunnel magnetoresistance (TMR) sensors have been recognized as a cost-effective alternative for measuring magnetocardiography (MCG) signals. However, their relatively high noise levels and susceptibility to contamination limit their practical clinical applications. To address these challenges, we propose a novel Multi-Level Gated U-Net (MGU-Net) model specifically designed for denoising long sequential MCG signals obtained from TMR sensors. The MGU-Net leverages the U-Net architecture to learn hierarchical representations, integrated with a novel Gated Linear Unit (GLU) module to capture the periodic pattern of Q, R, and S wave complex (QRS complex) from MCG. This design enhances periodic cardiac signatures and suppresses irregular noise components through adaptive gating mechanisms. We have developed a TMR-based MCG system and collected both simulated and real MCG data in a magnetically shielded environment. The results show that our method improve signal-to-noise ratio (SNR) from -2.142 dB to 10.505 dB on the simulated MCG dataset and from 3.958 dB to 14.514 dB on the real dataset, surpassing other state-of-the-art methods. Our model successfully recovers subtle P-wave and T-wave features from the noisy signals, illustrating a promising direction of using TMR-based systems for potential practical clinical applications.

Keywords: Magnetocardiography (MCG) · Denoising · Tunnel Magnetoresistance · Gated Linear Unit

1 Introduction

Magnetocardiography (MCG) has emerged as a critical non-invasive diagnostic modality for analyzing cardiac electrical activity through its associated magnetic field patterns. Current MCG measurement technologies primarily rely on

*Contributed equally

superconducting quantum interference devices (SQUIDs) [3] or optically pumped magnetometers (OPMs)[1], each presenting distinct advantages and limitations. SQUID systems demonstrate exceptional sensitivity with ultra-low noise levels ($\sim$2-5 fT/$\sqrt{\text{Hz}}$) [20][15] and superior low-frequency stability, making them the gold standard for clinical MCG applications. However, their operational dependence on liquid helium cooling systems and substantial equipment costs ($\sim$ \$1M) significantly limit widespread clinical adoption. OPM technology offers comparable magnetic field resolution to SQUIDs while eliminating cryogenic requirements, but introduces new challenges including complex optical system configurations, precise alkali vapor cell management, and mandatory magnetic shielding for optimal performance. These technical demands result in increased maintenance complexity and operational costs that hinder practical implementation. In comparison, tunnel magnetoresistance (TMR) sensors with miniaturized semiconductor designs have been considered as a cost-effective alternative technique for measuring MCG [6][14]. However, their relatively high noise ($\sim$2–200 pT/$\sqrt{\text{Hz}}$) [10][14] and susceptibility to noise contamination restrict their practical clinical applications.

To obtain clean magnetocardiography (MCG) signals using TMR sensors, efforts have been made to use traditional methods such as digital filters [16], AC modulation [22], and empirical mode decomposition (EMD) [14]. However, their effectiveness remains limited due to inherent constraints in handling non-stationary noise and preserving subtle cardiac features. Recent advances in deep learning have shown promise for electrocardiogram (ECG) denoising through architectures like DeepFilter (a multipath convolutional network) [17], DeScoD-ECG (diffusion-based model) [12], and Transformer-based TCDAE [2]. However, critical differences exist between ECG and MCG noise profiles: ECG denoising primarily targets baseline drift (0.05-2Hz), electrode motion artifacts (0.1-10 Hz), and muscle noise (5-500 Hz), whereas TMR-based MCG systems predominantly exhibit 1/f electrical noise spanning 0.1-100 Hz with non-uniform spectral decay. Current deep learning approaches achieve a significant improvement on ECG datasets, but demonstrate suboptimal performance when applied to MCG signals due to mismatched noise characteristics and sensor-specific artifacts.

In this paper, we proposed an Multi-Level Gated U-Net (MGU-Net) model specifically for denoising MCG signals acquired by TMR sensors. We leverage the U-Net architecture to perform multi-scale feature extraction, combined with a novel gated linear unit (GLU) to enhance cardiac feature extraction and attenuate non-periodic noise by capitalizing on the periodicity inherent in the MCG signal. The proposed model has an excellent performance on the task of denoising TMR-based MCG signals, which opens up a promising direction of using TMR-based systems for potential practical clinical applications.

2 Method

We start with an analysis of noise characteristics in MCG signals. Fig. 3(a) displays an episode of single-channel raw MCG signal acquired using the TMR sen-

sor. As shown, the noise exhibits random fluctuations with irregular amplitude and frequency variations, indicative of white noise originating from electronic systems (e.g., thermal agitation in sensor components) and 1/f noise inherent to TMR sensors in low-frequency domains. Crucially, subtle cardiac features such as P-waves and T-waves are mostly obscured by noise, with only the R-peak component faintly observable in specific segments. This observation highlights the challenge of extracting clean signals from a single cardiac cycle. To address this, we construct datasets with samples of around 10-second length to provide sufficient periodic information of Q, R, and S wave complex (QRS complex) for the model to learn. For processing such long-sequence signals, our model incorporates two critical design principles:

Hierarchical Feature Extraction: Direct processing of full-length MCG sequences (typically containing ∼10 cardiac cycles) poses significant computational challenges due to their extended duration and morphological complexity. To address this, we implement a multi-scale feature extraction strategy that progressively learns both localized waveform details and global contextual patterns. Drawing inspiration from successful applications in high-resolution image processing [21][13], our framework employs a U-Net architecture to facilitate comprehensive feature learning across multiple temporal resolutions, ensuring robust representation of both transient cardiac events and sustained rhythm characteristics.

Periodic Pattern Recognition: The most distinctive characteristic of MCG signals lies in the periodically occurring QRS complexes within extended signal sequences. To effectively utilize this periodicity for enhanced cardiac feature extraction and non-periodic noise suppression, our model incorporates a GLU designed specifically to capture long-range dependencies and reinforce these recurring patterns. This architecture enables systematic amplification of periodic cardiac signatures while attenuating irregular noise components through adaptive gating mechanisms.

2.1 The U-Net Architecture

As it can be seen in Fig. 1(a) Our model employs a U-Net architecture integrated with GLUs at multiple hierarchical levels to capture periodic patterns for denoising. The network incorporates two GLU variants: Competitive Gating (CG) modules and Noise Gating (NG) modules. The input signal first traverses an NG module, expanding its channel dimension from 1 to 64. Subsequent processing involves four downsampling stages, each comprising a ResBlock, a CG module, and a downsampling layer. Each downsampling operation halves the signal length while doubling the channel dimension.

At the bottleneck stage, the compressed signal undergoes feature aggregation across hierarchical layers, enabling the learning of high-level representations. Following this, three upsampling stages progressively restore spatial resolution. During upsampling, features from corresponding encoder stages are concatenated with the decoder pathway, followed by processing through ResBlock and CG

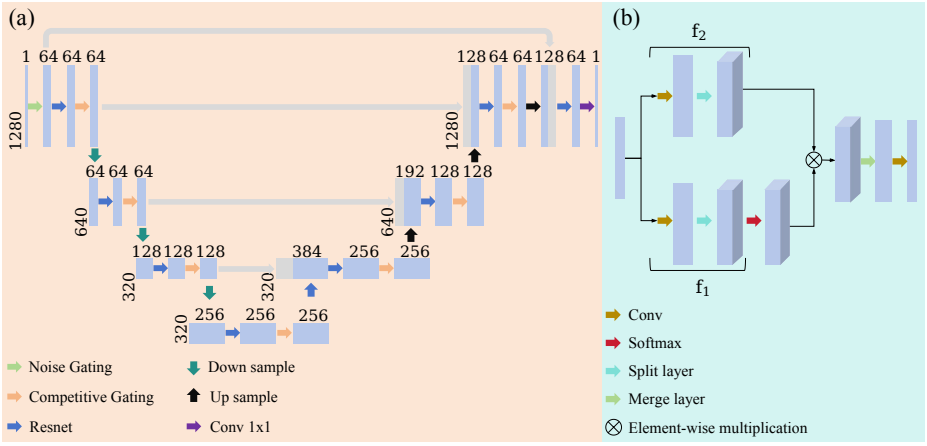

Fig. 1. Structure of the proposed Multi-Level Gated U-Net model. (a) The whole architecture (b) The GLU module.

modules . This multi-scale feature fusion mechanism preserves critical temporal relationships through skip connections while mitigating information loss.

After the final upsampling stage, the signal dimension reaches 64 × 1280. A 1×1 convolutional layer then reduces the channel dimension to 1, yielding the denoised output 1 × 1280. In this model, the convolutions were implemented with kernel sizes of 9 for the resnet block, 7 for the gating branch, and 4 for down/upsampling and followed by RMSNorm and SiLU activation. This hierarchical design achieves efficient information compression and reconstruction, balancing computational efficiency with robust feature extraction across transient cardiac events and sustained rhythm patterns.

2.2 The GLU module

An intuitive approach for learning the periodic patterns in MCG signals is to employ the self-attention(SA) mechanism [18], which effectively models long-range dependencies to capture amplitude variations and inter-cycle interval regularity. Given an input MCG feature sequence $X_{\text{in}} \in \mathbb{R}^{T\times D}$, where T denotes the sample length and D the feature dimension, self-attention transforms X_{in} through learnable parameter matrices $W_Q, W_K, W_V \in \mathbb{R}^{D\times d_k}$ to obtain query (Q), key (K), and value (V) matrices $Q = X_{in}W_Q$, $K = X_{in}W_K$, $V = X_{in}W_V$. The output is computed as:

$$X_{\text{out}} = \text{softmax}\left(\frac{QK^\top}{\sqrt{d_k}}\right)V \tag{1}$$

We replace the $QK^\top$ computation with learnable linear projections, resulting a gated linear unit (GLU)[4]:

$$X_{\text{out}} = \sigma\left(f_1(X_{\text{in}};\theta_W)\right) \odot f_2(X_{\text{in}};\theta_V) \tag{2}$$

where f_1 and f_2 are linear mappings parameterized by θ_W and θ_V, respectively, and σ denotes the activation function. The replacement of SA with GLU is primarily driven by the periodic nature of MCG signals. As MCG exhibits strong self-correlation patterns and amplitude-dependent dependencies, GLU's gating mechanism (via element-wise multiplication of two linear projections) inherently captures these global periodic features. In contrast, SA requires separate computation of Query (Q) and Key (K) introducing redundant parameters (e.g., Q/K projection layers), which could lead to suboptimal convergence of the model.

As shown in Fig. 1(b), both f_1 and f_2 utilize the same pipeline to process X_{in}. Each pipeline comprises a convolutional layer followed by a multi-head split layer. The standard GLU with σ as the softmax activation function is called competitive gating module in our paper, as it calculates gating weights globally through Softmax to capture the global dependencies of the signal, allowing periodic features such as QRS complexes to receive higher weights throughout the sequence. In the first layer, the σ is implemented as the sigmoid function, as it is designed to perform preliminary processing of MCG signals with low signal-to-noise ratio (SNR) by suppressing random noise and enhancing key features. We call this variant of standard GLU as noise gating module. Our code is available at https://github.com/YorkXingZeyu/MCG-denoising-project.git

3 Experiments

3.1 Data acquisition

TMR-based MCG system: We designed a TMR sensor consisting of thousands of MTJs (Fig. 2(a)) connected in series and parallel for MCG signal acquisition. Four TMR sensors were arranged in a Wheatstone bridge configuration (Fig. 2(b)) and encapsulated for protection to form a complete TMR sensor. To amplify the signals, we designed and fabricated an ultra-low noise amplification circuit board (Fig. 2(c)). The equivalent input noise at 1 Hz is approximately 10 nV/$\sqrt{\text{Hz}}$, which is lower than the noise of the TMR sensor itself. The TMR sensor is connected the amplification board to form a TMR probe. Additionally, we created a four-channel adapter module (Fig. 2(d)) to connect the TMR probe and output the signals to the DAQ for real-time data visualization and recording on a PC. The overall system noise level was reduced to 3-5 pt/$\sqrt{\text{Hz}}$ through optimized system design, enabling high-sensitivity detection of MCG signals.

Simulated MCG dataset: We developed a simulated magnetic signal generation system (Fig. 2(e)) that uses a Helmholtz coil to convert electrical signals from an arbitrary waveform generator (AWG) into magnetic signals. Inside a magnetically shielded barrel, TMR probes capture the magnetic field generated by the Helmholtz coil, with the magnetic field strength serving as the ground truth. The input signals to the AWG are derived from preprocessed data in the Kiel Cardio database[7] from seven healthy male volunteers. The primary types of noise of clean signals from Kiel Cardio DB are thermal noise, optical system noise, and shot noise ($<$15 fT/$\sqrt{\text{Hz}}$), which are negligible after filtering, in comparison to the captured noise from the TMR system with levels around

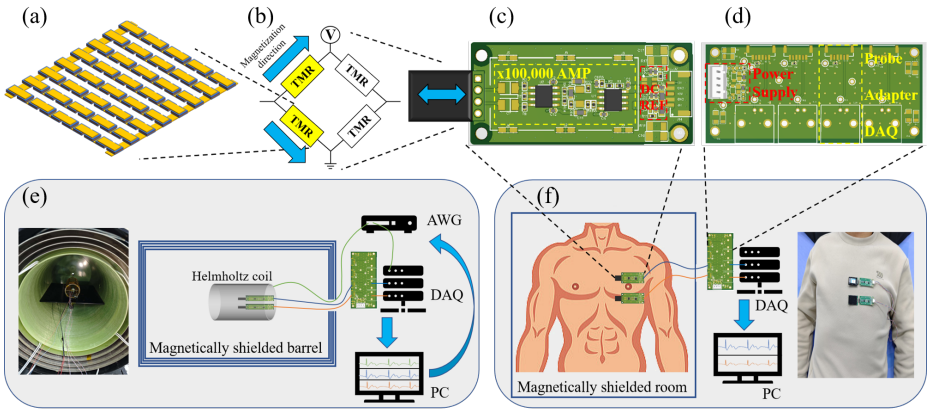

Fig. 2. TMR-based MCG system and experiment setups. (a) A TMR sensor array composed of magnetic tunnel junctions (MTJs). (b) Four TMR elements in a Wheatstone bridge configuration for converting magnetic signals into differential voltage. (c) TMR sensor integrated with a 100dB amplifier and power supply circuit. (d) 4-channel adapter module connecting the power supply and amplifier to the data acquisition system (DAQ). (e) The experiment setup for obtaining simulated data. (f) The experiment setup for obtaining real data.

5 pT/$\sqrt{\text{Hz}}$. The data is segmented into 10-second samples. Each sample contains several complete cardiac cycles, with the peak-to-peak range linearly scaled between 80 pT and 200 pT. A total of 6957 samples were obtained.

Real MCG dataset: The experiment was conducted in a magnetically shielded room. Ten healthy male subjects aged between 18 and 35 years participated in the experiment. During data collection, each one remained stationary in a supine position (Fig. 2(f)), and probes were placed above their chest to acquire MCG signals. This study adheres to the ethical guidelines of the Chinese Academy of Sciences Institute of Automation (CASIA), China and was approved by Human Subjects Research Ethics Review Committee of CASIA (Ref: IA21-2302-430203). The acquired signals were filtered using a 1-35 Hz bandpass filter. Subsequently, the signals were averaged over 101 cardiac cycles, using the R-wave peak as a reference to obtain the ground truth. The data from the TMR sensor were then segmented into 10-second episodes, each containing multiple complete cardiac cycles. A total of 2868 samples were obtained.

3.2 Results

We compared MGU-Net with other methods based on four metrics, which are Sum of the Square of the Distances (SSD), Maximum Absolute Distance (MAD), Cosine Similarity (Cosine Sim), and Signal-to-Noise Ratio (SNR) [12]. The "Baseline" in Table 1 was implemented by obtaining an average of the cardiac cycles in a sample and then rearranging it to align with the peaks to form the same

Table 1. Comparison on the Simulated and MCG Real Datasets.

Datasets	**Simulated MCG Dataset**				**Real MCG Dataset**			
Metrics	**SNR ↑**	**SSD ↓**	**MAD ↓**	**Cosine Sim ↑**	**SNR ↑**	**SSD ↓**	**MAD ↓**	**Cosine Sim ↑**
FIR Filter[9]	-0.5462	6.5051	0.2762	0.6139	4.3598	4.9430	0.2185	0.8231
IIR Filter[9]	-0.5752	6.5444	0.2763	0.6179	4.2813	4.9999	0.2215	0.8347
EMD[11]	-1.2439	7.7633	0.2992	0.5732	3.6089	5.8973	0.2370	0.8195
EEMD[19]	0.4674	5.3164	0.2648	0.5884	3.9274	5.4687	0.2312	0.8306
VMD[5]	0.2766	5.6047	0.3026	0.4544	4.5735	4.7173	0.2179	0.8308
APR-CNN [8]	7.5702	1.0901	<u>0.1993</u>	<u>0.9097</u>	10.0929	<u>1.0469</u>	<u>0.1261</u>	0.9485
TCDAE[2]	2.6863	3.2524	0.2819	0.6683	5.9516	3.4829	0.2118	0.8509
RA-LENet[23]	2.1276	3.8124	0.3207	0.6946	6.3643	2.3523	0.2101	0.8756
DeScoD[12]	<u>7.7682</u>	<u>1.0632</u>	0.2251	0.8988	8.3049	2.0278	0.1593	0.9214
Baseline	4.2304	2.2240	0.2351	0.7968	<u>11.2663</u>	1.0571	0.1470	<u>0.9530</u>
Our Model	**10.5051**	**0.5709**	**0.1511**	**0.9465**	**14.5143**	**0.4717**	**0.0699**	**0.9815**

length as the original sample. Five-fold cross validation was conducted, where 0.1 of the training data were used for validation. All the deep-learning models except for DeScoD were trained for 200 epochs with early stopping and a learning rate of 0.0001. For DeScoD, a higher learning of 0.001 was used according to its original paper. A batch size of 32 was used for all the models. For all the deep-learning based models, we use the Adam optimizer with a learning rate of 0.0001 and batch size was set as 32. The optimization process was guided by the mean squared error (MSE) loss.

As it can be seen in Table 1, the proposed MGU-Net method outperforms all the other methods based on all of the four evaluation metrics. The first five traditional methods have incremental improvement on the data due to their inherent constraints in handling non-stationary noise and preserving subtle cardiac features. All of the comparison methods fail to outperform Baseline on the Real Dataset based on SNR, which indicates that current state-of-the-art methods fails to capture the periodic pattern in the noisy MCG signals. In comparison, our proposed model combining U-net structure with GLU module can successfully capture essential information for denoising periodical MCG signals.

As shown in Fig. 3, the Baseline fails to filter the high-frequency noise from the signal. DeScoD and APR-CNN fail to restore the QRS complex in several cardical cycles. In contrast, only our proposed MGU-Net model achieves the best performance in the denoising task. It accurately restores every QRS complex with high fidelity. Low-amplitude features (like P-waves and T-waves), are also clearly accurately restored in the sample. In aspect of clinical utility, MGU-Net is lightweight and efficient, with 16.13 million parameters, 6.6 GFLOPs, and a real-time inference speed of 5.06 ms (versus DeScoD: 5.31 ms and APR-CNN: 6.42 ms) per sample on an RTX 4090 GPU, making it competitive for practical deployment.

Ablation Study In the ablation study (Table 2), we compare the impact of CG and NG on model performance. Using CG alone improves SNR of the plain model by 1.71 dB (Simulated) and 2.85 dB (Real). Using NG alone results in a more significant SNR improvement of the plain model (3.22 dB for Simulated and

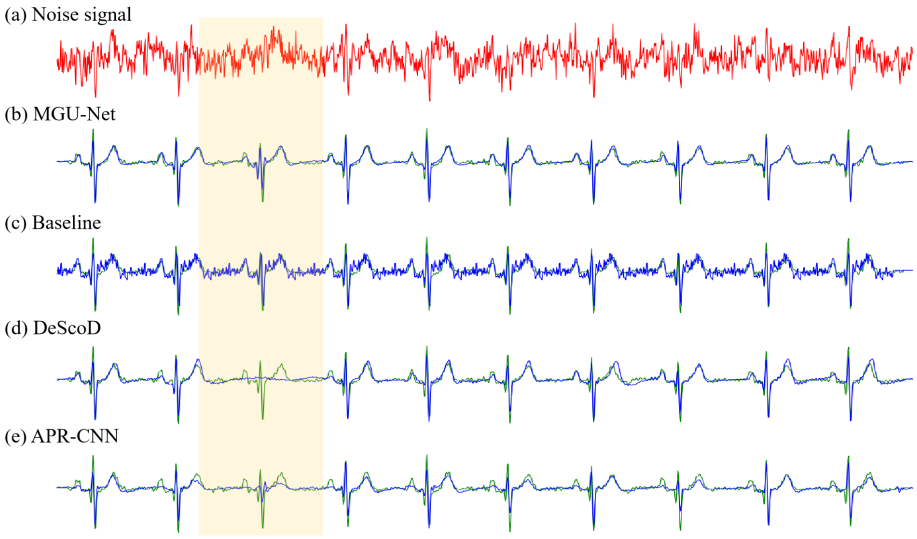

Fig. 3. Denoising performance of different models on a single sample from the simulated dataset. The red line represents the noisy input signal, the green line represents the ground-truth signal, and the blue line represents the denoised signal. (a) The original noisy MCG signal. (b) Denoised signal by MGU-Net. (c) Denoised signal by Baseline. (d) Denoised signal by DeScoD. (e) Denoised signal by the APR-CNN model.

6.16 dB for Real), with reductions in SSD and MAD, indicating NG effectively suppresses noise. Combining CG and NG yields the best results: SNR improves to 12.65 dB (Simulated) and 10.56 dB (Real), demonstrating the synergistic effect of both modules. The performance of using SA is inferior to that of using the combination of CG and NG.

4 Conclusion

This paper presents a novel deep learning model named MGU-Net for denoising MCG signals acquired using TMR sensors. By integrating noise gating and competitive gating mechanisms to capture the periodic patterns, MGU-Net effectively suppresses noise while preserving key cardiac features of MCG. Experimental results demonstrate that our method outperforms state-of-the-art denoising models in recovery of low-amplitude P-wave and T-waves, which are clinically essential for diagnosing arrhythmias, myocardial ischemia, and other cardiac abnormalities, in a high-noise real MCG recording. This work provides a foundation for the broader application of TMR-based MCG in clinical diagnostics and pathological analysis, offering a cost-effective and scalable alternative for cardiac monitoring.

Our current study was conducted only on a limited of subjects, primarily healthy individuals with normal MCG forms. To address the limitation, we will

Table 2. Ablation studies of the proposed model on the simulated and real MCG datasets. The impact of Competitive Gating (CG) and Noise Gating (NG) modules are evaluated.

Dataset	CG	NG	SA	SSD ↓	MAD ↓	Cosine Sim ↑	SNR Input	SNR Output ↑	SNR Improvement ↑
Simulated MCG Dataset	×	×	×	1.6518	0.2366	0.8377	-2.1423	5.6854	7.8277
	✓	×	×	1.1218	0.2037	0.8932	-2.1423	7.3937	9.5360
	×	✓	×	0.8246	0.1666	0.9223	-2.1423	8.9113	11.0536
	×	×	✓	0.6564	0.1664	0.9363	-2.1423	9.8074	11.9498
	✓	✓	×	**0.5709**	**0.1511**	**0.9465**	-2.1423	**10.5051**	**12.6474**
Real MCG Dataset	×	×	×	3.3924	0.2775	0.8213	3.9576	4.8834	0.9258
	✓	×	×	2.1686	0.2356	0.9128	3.9576	7.7366	3.7790
	×	✓	×	1.0615	0.1487	0.9575	3.9576	11.0431	7.0855
	×	×	✓	0.5118	0.1096	0.9769	3.9576	14.1827	10.2251
	✓	✓	×	**0.4717**	**0.0699**	**0.9815**	3.9576	**14.5143**	**10.5567**

expand the scope of future research by incorporating a more diverse cohort of participants, including patients with cardiac diseases. Accordingly, we will prioritize improving the model's stability and consistency (e.g., exploration on multi-loss frameworks) across different populations.

Acknowledgments. This work was supported in part by the National Natural Science Foundation of China (62327805, 62336007) and the STI2030-Major Projects (2021ZD0200201).

Disclosure of Interests. The authors have no competing interests to declare that are relevant to the content of this article.

References

1. Alexandrov, E.B., Bonch-Bruevich, V.A.: Optically pumped atomic magnetometers after three decades. Optical Engineering **31**(4), 711–717 (1992)
2. Chen, M., Li, Y., Zhang, L., Liu, L., Han, B., Shi, W., Wei, S.: Elimination of random mixed noise in ecg using convolutional denoising autoencoder with transformer encoder. IEEE Journal of Biomedical and Health Informatics (2024)
3. Clarke, J.: Squid fundamentals. In: SQUID sensors: fundamentals, fabrication and applications, pp. 1–62. Springer (1996)
4. Dauphin, Y.N., Fan, A., Auli, M., Grangier, D.: Language modeling with gated convolutional networks. In: International conference on machine learning. pp. 933–941. PMLR (2017)
5. Dragomiretskiy, K., Zosso, D.: Variational mode decomposition. IEEE transactions on signal processing **62**(3), 531–544 (2013)
6. Fujiwara, K., Oogane, M., Kanno, A., Imada, M., Jono, J., Terauchi, T., Okuno, T., Aritomi, Y., Morikawa, M., Tsuchida, M., et al.: Magnetocardiography and magnetoencephalography measurements at room temperature using tunnel magnetoresistance sensors. Applied Physics Express **11**(2), 023001 (2018)
7. Goldberger, A.L., Amaral, L.A., Glass, L., Hausdorff, J.M., Ivanov, P.C., Mark, R.G., Mietus, J.E., Moody, G.B., Peng, C.K., Stanley, H.E.: Physiobank, physiotoolkit, and physionet: components of a new research resource for complex physiologic signals. circulation **101**(23), e215–e220 (2000)

8. He, Z., Liu, X., He, H., Wang, H.: Dual attention convolutional neural network based on adaptive parametric relu for denoising ecg signals with strong noise. In: 2021 43rd Annual International Conference of the IEEE Engineering in Medicine & Biology Society (EMBC). pp. 779–782. IEEE (2021)
9. Heinonen, P., Saramaki, T., Malmivuo, J., Neuvo, Y.: Periodic interference rejection using coherent sampling and waveform estimation **31**(5), 438–446 (1984)
10. Hou, Y., Wang, D.F., Itoh, T.: Maximizing modulation efficiency to minimize 1/f noise in magnetoresistance. Measurement **207**, 112396 (2023)
11. Huang, N.E., Shen, Z., Long, S.R., Wu, M.C., Shih, H.H., Zheng, Q., Yen, N.C., Tung, C.C., Liu, H.H.: The empirical mode decomposition and the hilbert spectrum for nonlinear and non-stationary time series analysis. Proceedings of the Royal Society of London. Series A: mathematical, physical and engineering sciences **454**(1971), 903–995 (1998)
12. Li, H., Ditzler, G., Roveda, J., Li, A.: Descod-ecg: Deep score-based diffusion model for ecg baseline wander and noise removal. IEEE Journal of Biomedical and Health Informatics (2023)
13. Liang, J., Timofte, R., Yi, Q., Liu, S., Sun, L., Wu, R., Zhang, X., Zeng, H., Zhang, L., Huang, Y., et al.: Ntire 2024 restore any image model (raim) in the wild challenge. In: Proceedings of the IEEE/CVF Conference on Computer Vision and Pattern Recognition. pp. 6632–6640 (2024)
14. Lu, Z., Ji, S., Yang, J.: Measurement of t wave in magnetocardiography using tunnel magnetoresistance sensor. Chinese Physics B **32**(2), 020703 (2023)
15. Maslennikov, Y.V., Primin, M., Slobodchikov, V.Y., Khanin, V., Nedayvoda, I., Krymov, V., Okunev, A., Moiseenko, E., Beljaev, A., Rybkin, V., et al.: The dc-squid-based magnetocardiographic systems for clinical use. Physics Procedia **36**, 88–93 (2012)
16. Oogane, M., Fujiwara, K., Kanno, A., Nakano, T., Wagatsuma, H., Arimoto, T., Mizukami, S., Kumagai, S., Matsuzaki, H., Nakasato, N., et al.: Sub-pt magnetic field detection by tunnel magneto-resistive sensors. Applied Physics Express **14**(12), 123002 (2021)
17. Romero, F.P., Piñol, D.C., Vázquez-Seisdedos, C.R.: Deepfilter: An ecg baseline wander removal filter using deep learning techniques. Biomedical Signal Processing and Control **70**, 102992 (2021)
18. Vaswani, A., Shazeer, N., Parmar, N., Uszkoreit, J., Jones, L., Gomez, A.N., Kaiser, Ł., Polosukhin, I.: Attention is all you need. Advances in neural information processing systems **30** (2017)
19. Wu, Z., Huang, N.E.: Ensemble empirical mode decomposition: a noise-assisted data analysis method. Advances in adaptive data analysis **1**(01), 1–41 (2009)
20. Yang, K., Chen, H., Kong, X., Lu, L., Li, M., Yang, R., Xie, X.: Weakly damped squid gradiometer with low crosstalk for magnetocardiography measurement. IEEE Transactions on Applied Superconductivity **26**(8), 1–5 (2016)
21. Zamir, S.W., Arora, A., Khan, S., Hayat, M., Khan, F.S., Yang, M.H.: Restormer: Efficient transformer for high-resolution image restoration. In: Proceedings of the IEEE/CVF conference on computer vision and pattern recognition. pp. 5728–5739 (2022)
22. Zhao, W., Tao, X., Ye, C., Tao, Y.: Tunnel magnetoresistance sensor with ac modulation and impedance compensation for ultra-weak magnetic field measurement. Sensors **22**(3), 1021 (2022)
23. Zhu, Y., Zhu, D., Liu, J.: Ra-lenet: R-wave attention and local enhancement for noise reduction in ecg signals. In: 2024 International Joint Conference on Neural Networks (IJCNN). pp. 1–9. IEEE (2024)